Digital Video Transmission System with Pilot Aided C-OFDM

Yasuo Harada, Hiroshi Hayashino, Yasuhiro Uno, Tomohiro Kimura
Hitoshi Mori, Manager
Information & Communications Technology Laboratory
Matsushita Electric Industrial Co. Ltd.

ABSTRACT

A digital video transmission system is proposed that uses a pilot-aided Coded Orthogonal Frequency Division Multiplexing (COFDM) scheme with multiple carriers which are individually modulated using QAM. Multiple MPEG video channels are supported within a 6MHz band. OFDM is known for its multipath mitigation effect.

The technique is described from an implementation point of view, addressing such issues as equalization of channel characteristics, AFC, AGC and timing synchronization, which are critical for realizing the system. Trellis decoding is also discussed with respect to equalizing the channel characteristics, which improves the bit error rate performance. The performance of the system are shown by the computer simulation.

1. INTRODUCTION

Digital video transmission schemes using QAM and VSB have been proposed recently[1][2].

CATV transmission line has reflections on the channel. The performance is degraded by channel impairments such as reflections and impedance mismatches. OFDM is a robust technology for overcoming the reflections. We propose a digital transmission system using OFDM that achieves good bit error performance using Trellis-Coded Modulation and Reed Solomon code.

2. OUTLINE of TRANSMISSION SYSTEM

Figure 1 shows the outline of the transmitter of the proposed system. Four video programs with MPEG 2 coded digital TV source are accommodated. These video source data are multiplexed into a single stream in an I/F board.

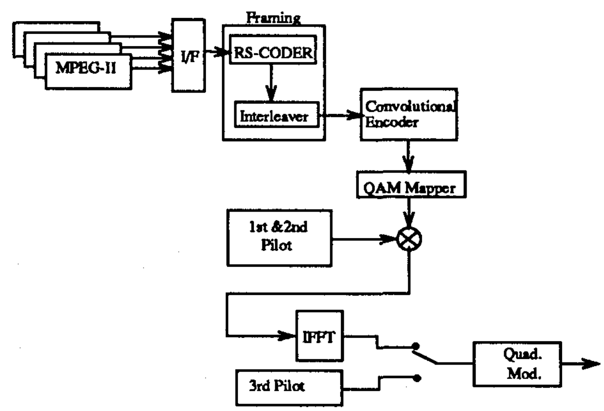

Figure .1 Configuration of OFDM System

The multiplexed data is fed into a Reed Solomon encoder. We use an RS(208,188) code with 10 symbol error correction capability. The output of the Reed Solomon encoder is interleaved symbol-by-symbol of the RS code words. The output data of the interleaver is fed into a convolutional encoder. The convolutional encoder processes the input symbols five-bit at a time. Encoded 6-bit vectors are mapped into QAM vectors. A single OFDM symbol contains 512 carriers, with 10 KHz carrier spacing, each of which is modulated using

64-QAM. 512 symbols of QAM for 512 carriers of each symbols are transferred to the time domain using an IFFT, resulting in a group modulating 512 QAM carriers.

A 1024 complex data IFFT which generates the baseband OFDM signal in the time domain. The time domain OFDM baseband complex data is converted into an IF signal by a quadrature modulator realized by a digital interpolation filter and multiplexing.

3. FRAME FORMAT

The frame structure is shown in Figure 2. The frame consists of three pilot symbols as preamble, and 4 data frames each of which has 52 OFDM symbols. The pilot symbols are inserted every 21.1 msec.

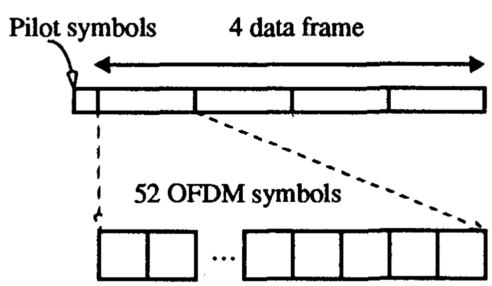

Figure .2 Frame structure

3.1 RS Error Correcting Code and Interleaving

We use a concatenation error correcting code with an RS code and Trellis-Coded Modulation for error control. The RS code is used for channel coding because it has good performance in burst error conditions, providing a reliable channel.

We choose an RS (208,188) code which can correct upto 10 symbols. Each symbol contains 8bits. The interleaving matrix design takes into consideration of the RS code length and the number of carriers in one OFDM symbol.

Figure 3 shows the interleaving matrix. The data frame consists of the interleaving matrix of 208 bytes by 80 RS code words, which corresponds to 128 carriers space interleaving depth. The interleaving spreads erroneous symbols up to 128 carriers consecutive errors. A whole OFDM symbol corrupted, only four symbols of any single Reed Solomon codeword may be corrupted, which can be completely corrected.

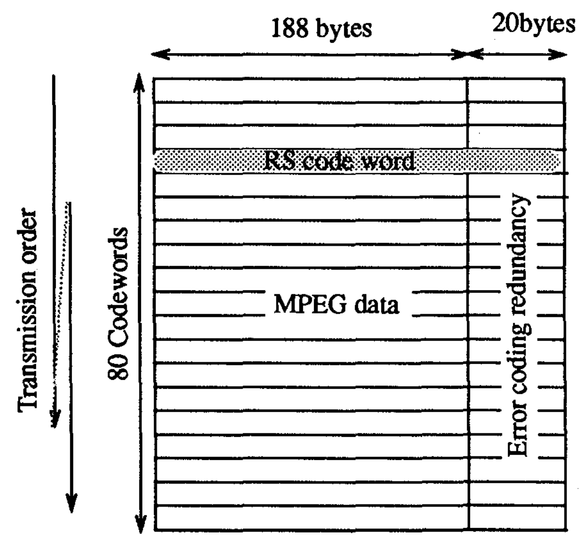

Figure .3 Interleaving matrix

3.2 Pilot Signal

We use pilot symbols to realize channel equalization, timing synchronization and frequency offset correction. Three pilot symbols are followed by 4 data frames. Each data frame is shown in Figure 3, which is the interleaving frame. The first pilot symbol is a null signal period and the second is a sweep signal and the third pilot symbol is an ASK signal which is modulated by a PN sequence.

The first symbol can be used for coarse

timing detection for the data frame, however symbol timing precision is realized by the third pilot symbol.

The second pilot symbol can be used to measure the channel characteristics. All components in a frequency band (5.12MHz) of the second pilot has the same level so that we can detect the channel characteristics with equal precision in a bandwidth. The details of the second pilot is shown in the AFC explanation below.

The third pilot symbol is an Amplitude Shift Keying, which can be used for both timing synchronization and frequency control of received signal.

4. TIMING SYNCHRONIZATION

The carrier in the third pilot is modulated by a PN code of length of 2^7-1, which is generated by 7 bit linear feed back registers. At the receiver, the envelope detection is used for demodulation of ASK signals modulated by the PN code.

The PN code has a very sharp auto-correlation over additive white gaussian noise of the channel. The PN code of length 127 gives approximately 21dB of code separation and hence can be detected in the channel with C/N of 21dB.

The output of the correlator gives the position of the preamble of the data frame, and the timing precision is the reciprocal of the clock rate of the PN code. We use 1.28MHz of the clock of the PN code, and the PN peak point can be detected by the precision of 0.78μsec.

The PN code is detected by a correlator which is used as a synchronization word detector. We use the synchronization word protection to achieve quick and secure acquisition, and to release a lock in the case of a false lock. For the backward sync-word protection, a sync-word with N-bit errors is allowed to set the lock. Once synchronization is achieved, we allow a sync-word with M-bit errors. This realizes the synchronization with data frame.

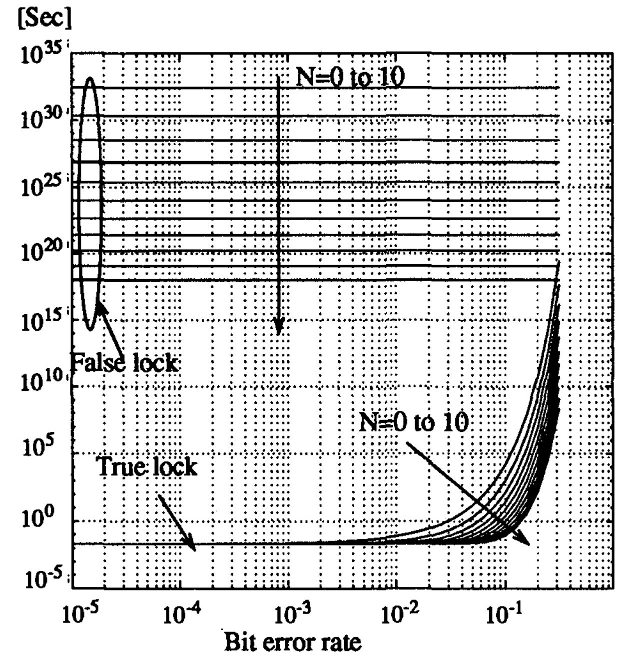

Figure .4 Lock up time for PN code synchronization

N and M can be determined by computer simulation. Figure 4 shows the time in seconds for the system to lock with N=0 to 10. When N is zero, no error is allowed, it takes approximately 27hours (10^5sec) to lock at a BER of 10^{-1} and 21msec to get the lock state. On the other hand a false lock happens every 10^{18} sec. with N=10, and 10^{31} sec. with N=0. We determine that if N is 10, a lock time is 21.1msec and a false lock occurs every 10^{18} second. Figure 5 shows the time in msec. for the system to unlock with M=10 to 20. When M is 20, a lock out occurs every 10^{15}sec. from a true lock, and it takes 10^{-6} sec. to unlock.

Another benefit of ASK signals, the received signal can be demodulated even with frequency offset. The advantage of this method is that the timing synchronization can be achieved with some frequency offset of the received signal. Moreover the ASK signal can provide the frequency information for the selection of the PLL-synthesizer frequency step of a tuner at the first stage of receiving.

Thus, channel selection for the tuner and symbol timing acquisition can be obtained by using the third pilot symbol which is the 2-Ary ASK signals.

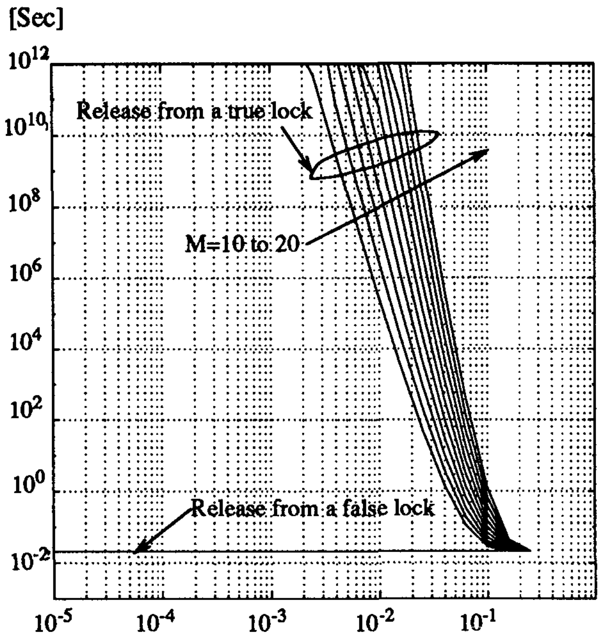

Figure .5 Release time of PN synchronization

5. DIFFERENTIAL DECODING and AUTOMATIC FREQUENCY CONTROL

We can use the second pilot for differential decoding and automatic frequency control. The second pilot symbol can be designed for differential decoding and frequency detection and gain control.

5.1 Description of the Second Pilot

The second pilot should be equal level for all carriers, which is an appropriate symbol for calculating the channel characteristics, in terms of a well-balanced dynamic range of equalization.

The pilot symbol should have a constant level in the time domain so that we can get a level information for AGC.

Considering the above features, we use the sweep signal shown in the Eq.-(1).

$$P(t) = exp(jwt)$$

$$= exp\left(j\pi\frac{F_s}{T_s}t^2\right) \quad (1)$$

,where Ts is the symbol duration and Fs is the nyquist bandwidth of OFDM symbols. The equation indicates that the pilot symbol has a constant level for AGC. The pilot symbol in a frequency domain can be written in this form;

$$P(f) = exp\left(j\pi\frac{T_s}{F_s}f^2\right). \quad (2)$$

We can see that the absolute values of each carrier's component are identical to *1.0*.

5.2 Differential Encoding and Detection

Suppose $S(f)$ is the transmitted OFDM symbol and $H(f)$ describes the channel characteristics. We can encode OFDM symbols differentially with the pilot symbol. The received symbol can be written in the following form;

$$R(f) = H(f)P(f)S(f). \quad (3)$$

and the received pilot symbol obtains the same channel characteristics and written in the form;

$$Rp(f) = H(f)P(f). \quad (4)$$

As in Figure 6, we can cancel the channel characteristics at the receiver by just dividing symbols by the received pilot symbol.

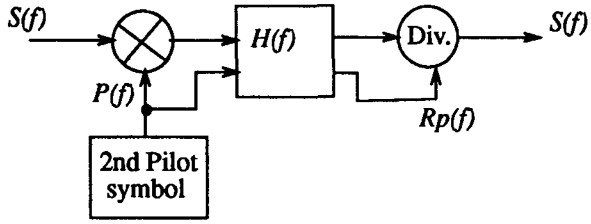

Figure .6 Differential Encoding and detection

5.3 Automatic Frequency Control

The receiver typically uses a PLL synthesizer for the tuner, where the tuner output frequency can be controlled by the synthesizer at 250 KHz step. The output signal of a tuner is converted into a complex baseband OFDM signal. Using an NCO we can correct the frequency offset. The frequency offset is obtained by manipulation of the second pilot symbol of Eq.-(1).

The phase is detected as

$$\Phi(t) = \pi\frac{Fs}{Ts}t^2 + 2\pi\varepsilon t \quad (5)$$

,where ε is frequency offset. Now the receiver holds the phase information of the second pilot symbol as an reference written as below:

$$\Phi_{ref} = \pi\frac{Fs}{Ts}t^2. \quad (6)$$

We subtract Eq.-(6) from Eq.-(5) and take the derivative of the result and obtain the linear function of the frequency offset.

$$\frac{d}{dt}\Delta\Phi = 2\pi\varepsilon \quad (7)$$

Using Eq.-(7) we can calculate the frequency offset and forward it to the NCO, forming an AFC loop. The additive white gaussian noise can be cancelled by averaging 8 frames of data.

Symbol error rate performance of the receiver was simulated and shown in Figure 7. We confirmed that the frequency offset is determined, even for a lower C/N. For the channel distortion, we could use the linear estimation with minimum mean-square.

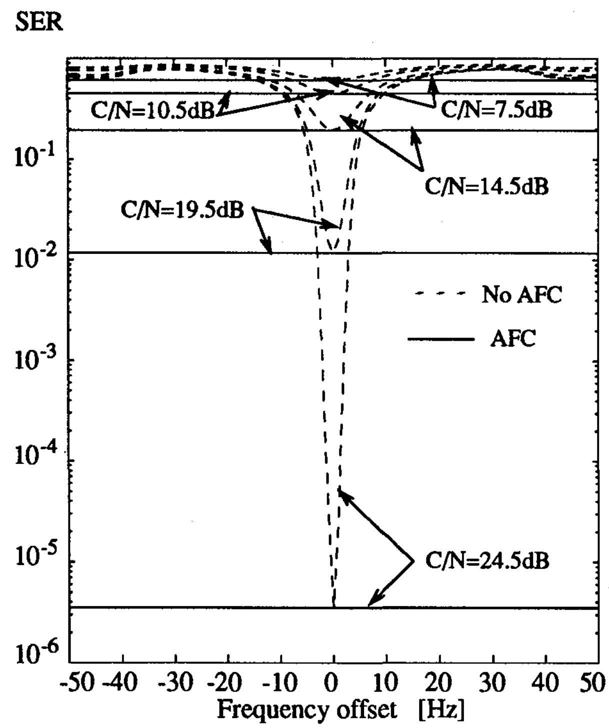

Figure .7 Symbol error rate versus frequency offset

6. BIT ERROR RATE PERFORMANCE of SYSTEM

6.1 Channel Model

The CATV channel is modeled from the view point of the physical channel architecture. Impedance mismatches of the trunk amplifiers generate the signal fluctuation within a bandwidth. In the case of OFDM signal, multiple carriers receives the signal fluctuations in the band. This can be caused by the delay version of the signals with different delay times. Usually we can use the model [2] considered for a cable architecture. For simplicity, however, we can use the model of a Rician channel, shown in Figure 8. The Rician model is applied to all carriers in a given bandwidth for each OFDM symbol. This model can be used to simulate the fluctuation of carriers in a given bandwidth due to reflections and losses of the channel.

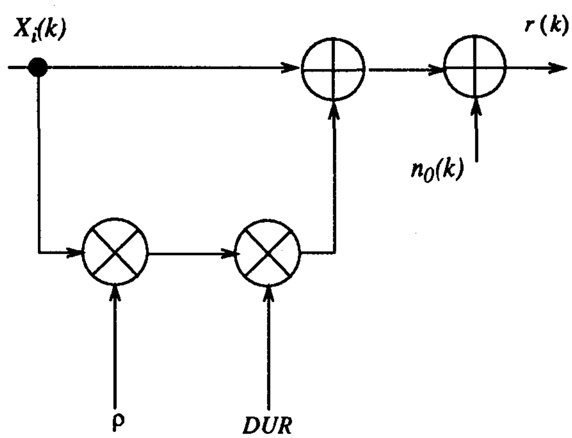

Figure .8 The channel model using Rician variables

This model of channel conditions is more severe than the condition of a real channel.

6.2 Differential Demodulation with the Second Pilot Symbol

As we discussed above, the second pilot symbol has equal level components of each OFDM carriers in a bandwidth. The pilot symbol receives the same distortion in a channel as the OFDM symbols, so each OFDM carrier multiplexed by the pilot symbol in the frequency domain, can be demodulated through division by the received pilot symbol which also contains the channel distortion. As a result we can cancel the distortion in the frequency domain by simple division by the pilot symbol. The performance of the bit error rate for coherent demodulation and differential demodulation of 64QAM/COFDM are compared in Figure 9 and Figure 10.

Figure 9 shows the bit error rate performance of coherent detection which is identical to the case of a single carrier 64QAM and 8VSB without equalization, at 0dB,12dB and 24dB of D/U. Figure 10 shows the bit error rate performance of a differential detector for 64QAM/COFDM with pilot symbols at 0dB,12dB and 24dB of D/U. We can notice the improvement of bit error rate performance by the channel characteristics equalization, which is differentially demodulated using the pilot symbol.

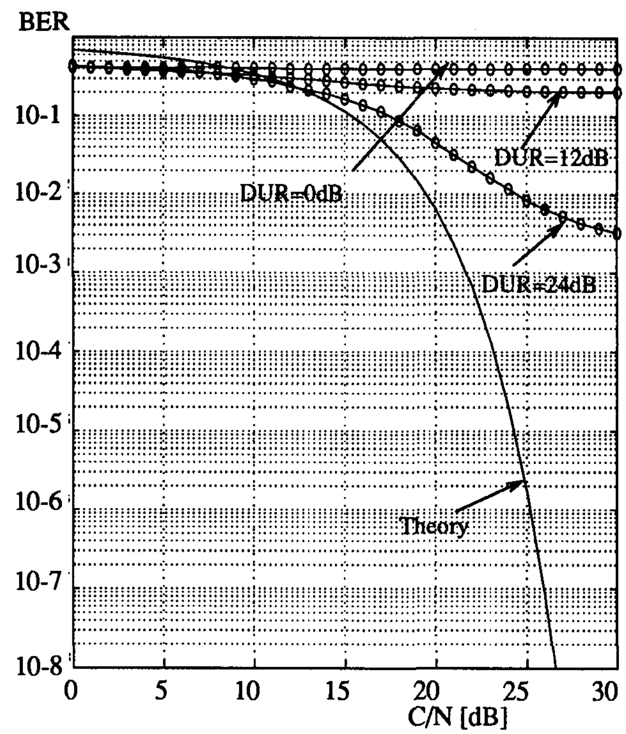

Figure .9 Bit error rate for 64QAM/OFDM by coherent detection at 0, 12, 24dB of DUR

6.3 Trellis Coded Modulation with Pilot Symbol

Trellis-Coded Modulation can provide high coding gain. We can further improve the coding

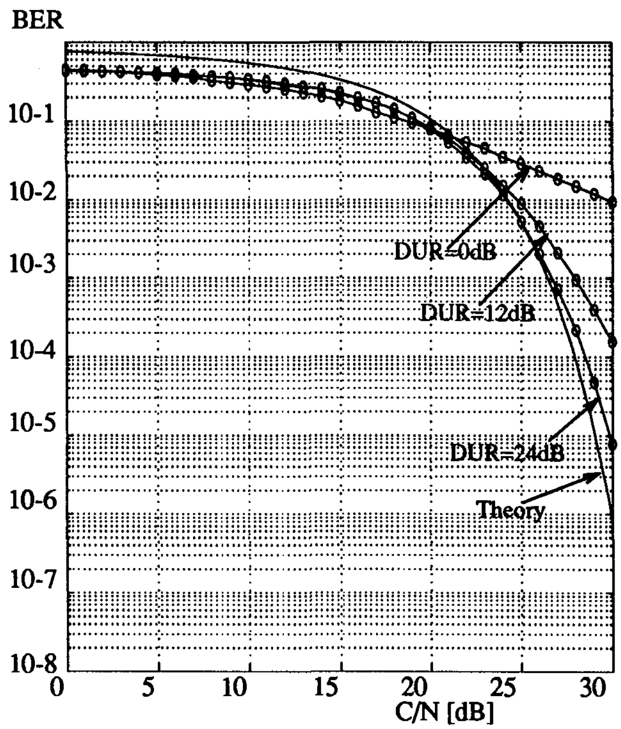

Figure .10 Bit error rate for 64QAM/COFDM with differential decoding by pilot symbols

gain of the system by using an RS code as an outer code. Trellis-Coded Modulation can be applied to correct the channel impairments, such as reflection and channel distortion, and was applied as an inner code. The OFDM signal contains the data in the frequency domain and we applied the trellis coding in both frequency domain and time domain.

The output data, from the interleaver, is encoded by the convolutional encoder shown in Figure 11 which is an Ungerboeck code.

As shown above, the pilot symbol can be used to equalize channel characteristics. We can also use this channel characteristic information in trellis decoding. The pilot symbol, containing channel characteristics, is extracted and forwarded to remodulate trellis reference metric. This remodulation technology can be used to realize both channel equalization and the metric calculation for trellis decoding. Figure 12 shows the bit error rate performance of 64QAM/COFDM using a pilot remodulation

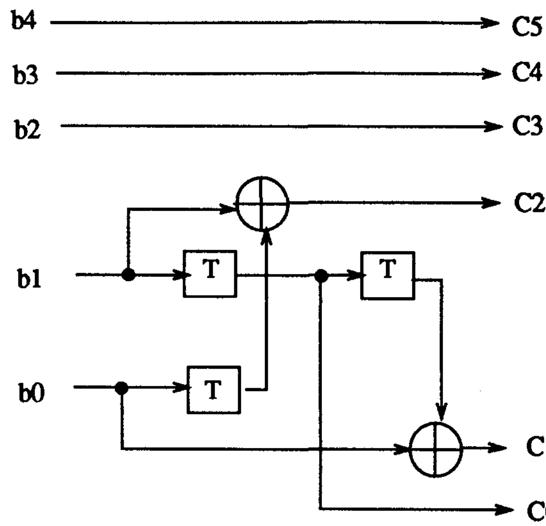

Figure .11 The convolutional encoder for 64 QAM/COFDM

metric in the trellis decoding, compared to the trellis decoding, to differential decoding at 12dB of D/U. Using trellis coded 64QAM/OFDM we can improve the bit error rate performance over pilot differential decoding of OFDM. The BER of COFDM is improved by 0.5dB by remodulation of the trellis metric. Although the improvement of C/N is not dramatic in this channel model, we can expect a further difference in performance when we have a null point or very small level in the received signal, which is always a problem for linear equalization. Using these methods we can avoid null point divergence of channel equalization.

By a concatenation of RS codes and trellis coded modulation, we can get a good performance of bit error rate as in shown Figure 12.

7. CONCLUSION

We have proposed a video transmission system with pilot aided COFDM. We have described the realization of the symbol timing acquisition and AFC, using pilot symbols. Further more we have shown pilot differential detection of Trellis-Coded Modulation which

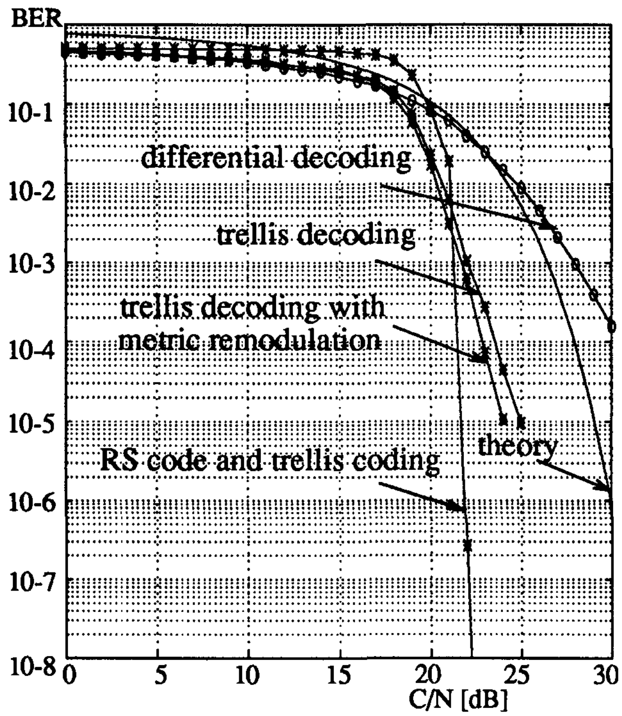

Figure .12 The comparison of bit error rate performance for differential decoding, trellis decoding, trellis decoding with metric remodulation, and the concatenation of RS code and Trellis-Coded Modulation with metric remodulation

improves the bit error rate performance. Concatenating RS codes and Trellis-Coded Modulation we can realize a good BER performance and a very high transmission rate of 22.8Mbps by using 512 QAM carriers. The capacity can be increased to 25Mbps using 560 QAM carriers. We are currently developing the system for laboratory experiment and we plan to compare the performance with the simulation results.

References

[1] R. B. Lee, "High data rate VSB Modem for Cable Applications Including HDTV," *NCTA Technical papers*, pp.274-279, May 1994

[2] K.Laudel *et.al.* "Performance of a 256QAM Demodulator/Equalizer in a Cable Environment," *NCTA Technical papers*, pp283-304, May, 1994

[3] P. H. Moose, "A technique for Orthogonal Frequency Division Multiplexing Frequency Offset Correction," *IEEE Trans. Commun.*, vol. 42 No.10 Oct. 1994

[4] S.B. Weinstein, "Data Transmission by Frequency-Division Multiplexing using the discrete fourier Trasform" *IEEE Trans. Commun.* vol com-19 No. 5 Oct. 1971

[5] G. Ungerboeck, "Channel coding with multilevel phase signal," *IEEE Trans. Information Theory*, vol. IT-28, pp. 55-67, Jan. 1982.

[6] G. Ungerboeck, "Trellis-Coded Modulation with Redundant Signal Sets - Part I: Introduction," *IEEE Communications Magazine*, vol. 25, no. 2, pp. 5-11, Feb. 1987.

[7] G. Ungerboeck, "Trellis-Coded Modulation with Redundant Signal Sets - Part II: State of the Art," *IEEE Communications Magazine*, vol. 25, no. 2, pp. 12-22, Feb. 1987.

[8] D. Divsalar and M. K. Simon, "The design of trellis coded MPSK for fading channel: performance criteria," *IEEE Trans. Commun.*, vol. 36, pp. 1004-1012, 1988.

[9] E. Biglieri *et.al.*, *Introduction to Trellis-Coded Modulation with Applications.* Macmillan Publishing Company, New York.

[10] S. Lin and D.J. Costello, Jr., *Error Control Coding: Fundamentals and Applications.* Englewood Cliffs, New Jersey, Prentice-Hall, 1983

[11] G.C. Clark, Jr. and J.B. Cain, *Error-Correction Coding for Digital Communication.* New York, Plenum Press, 1982.

[12] R. E. Blahut, *Theory and Practice of Error Control Codes.* Reading, MA: Addison- Wesley, 1983.